ISSN: 2277-9655
Impact Factor: 4.116
CODEN: IJESS7

IJESRT

INTERNATIONAL JOURNAL OF ENGINEERING SCIENCES & RESEARCH TECHNOLOGY

# A NUMERICAL MODEL FOR PREDICTING PERFORMANCE OF SOLAR PHOTOVOLTAIC, BIOMASS AND CHP HYBRID SYSTEM FOR ELECTRICITY GENERATION

**S. Sami and E. Marin**
[*] Research Center for Renewable Energy
Catholic University of Cuenca, Cuenca, Ecuador

**DOI**: 10.5281/zenodo.227935

## ABSTRACT

This paper presents a numerical model to simulate and predict the total power generated by a hybrid system composed of solar photovoltaic PV, and biomass-CHP integrated Combined Heat and Power. A numerical model based upon the energy conversion equations describing the aforementioned hybrid system was developed, coded and the results were analyzed and compared to experimental data. The predicted results of the model compared fairly with the experimental data under various conditions.

**KEYWORDS**: Hybrid System, Solar Photovoltaic, biomass, CHP, Modeling, Simulation, Validation experimental data.

## INTRODUCTION

Photovoltaic solar energy plants energy output is intermittent due to day/night cycles and also low irradiation periods during winter and cloudy days [1-8]. Although biomass power plants can operate continuously, they can have high initial cost, uncertain supply chain security and require bulk transportation [4]. Hybrid solar/biomass plants will become an increasingly attractive option as the price of fossil fuel and land continue to rise and the cost of solar thermal technology falls [5].

Renewable and nonconventional methods of power generation such as wind, solar, hydraulic, biomass, geothermal, thermal storage, waste heat recovery power generations and hybrid systems offer power supply solutions for remote areas that are not accessible to grid power supply. Hybrid renewable energy system is an integrated system of two or more renewable energy systems, that can complement each other, and provide higher quality and reliable power supply independent of the grid [4-5].

Mustafa [9] presented and discussed the electrification of rural area and a review of power standalone system such as; solar and hybrid, solar-wind, solar-hydro hybrid, solar-wind-diesel hybrid, and solar-wind-diesel-hydro/biogas. In addition, reference [9] presented and analyzed the viability and importance of solar energy use in global electrification. Another study was proposed by references [10-14] for implementation of hybrid systems in rural area disconnected from the grid. The study discussed two tri-hybridization processes. The tri-hybrid system included hydro-wind and Photovoltaic.

Incineration is one of the most effective biomass technologies for municipal waste disposal; however, it involves combustion pollution. Combustion gas is generated at the bed combustion where it passes through the furnace combustion chamber to complete the combustion process with all reactive gases. The main heat and mass transfer in the furnace combustion chamber are radiation, convection, conduction and moist content evaporation. These must be considered in incinerators study [13]. Various studies have focused on emission reduction in incinerators, Choi et al. [15]. A process simulation model for 2 ton/hr incinerator using a combined bed combustion and furnace heat transfer model, has been presented by Yang et al. [16, 17], however, the principal author [16], also presented a useful study on the improvement of operating conditions in waste incinerators using several engineering tools. In their study, one dimensional model for heat and mass balance, computational fluid dynamics CFD and global prediction model and observation model for dioxin is presented. Furthermore, sophisticated solutions dealing with

ISSN: 2277-9655
Impact Factor: 4.116
CODEN: IJESS7

incinerators such as real-time simulators for predictive performance of incinerators were presented by Gan et al [18].

Of a particular interest is the electrification of remote areas. A review of power stand-alone systems that are suitable for electrification of remote areas such as solar and hybrid, solar-wind, solar-hydro hybrid, solar-wind-diesel hybrid, and solar-wind-diesel-hydro/biogas hybrid systems have been presented and discussed in references [19-24]. Furthermore, the viability and importance of solar energy use in global electrification has been also presented and analyzed in reference [19]. Another study was proposed by Bhandari [11] for implementation in rural areas disconnected from the grid. The study discussed two tri-hybridization processes. The tri-hybrid system included hydro-wind and Photovoltaic. Furthermore, another PV and hydro-wind system has been suggested to supply uninterrupted power to a remote village in Ethiopia by Bekele and Tedesse [20]. This study used the code HOMER to optimize that hybrid system. In addition, other studies were presented on PV-wind-battery hybrid and PV-wind-diesel-battery hybrid intended for rural electrification in Malaysia and other areas [21-24].
On the other hand, the energy conversion equations describing the total power generated by a hybrid system of solar photovoltaic, wind turbine and hydraulic turbine were presented and integrated simultaneously by Sami and Icaza [7,23], for the purpose of validating this simulation model, the energy conversion equations were coded with MATLAB-V13.2.

This paper is concerned with the analysis of the main heat and mass transfer mechanisms encountered in PV thermal behavior and biomass furnace combustion chamber as well as performance of the biomass-CHP using Organic Rankine Cycle (ORC). A numerical simulation using one dimensional model is presented hereby to describe time-variation of the processes and performance of biomass incineration-CHP and as solar thermal PV.

## MATHEMATICAL MODELING

In the following sections, the energy conservation and conversion equations from each source of renewable energy to an electrical energy in the hybrid system under question are presented;

Biomass Incinerator:
This section presents the heat and mass transfer mechanisms for the incinerator furnace. The flue gas is released after the waste combustion bed. The radiation is the major heat transfer by-product because of the high temperature of the gas. The Heat released from the combustion bed is transferred to the ORC waste boiler by the thermal oil flow as shown in Figure.1. The other different heat transfer mechanisms present in the furnace are convective, evaporation and combustion. These heat transfer mechanisms must be taken into consideration in order to solve the energy conservation and conversion equations of the biomass incinerators process [15- 17 and 26];

$$Q_{adrin_{gas}} - Q_{adrout_{gas}} = Q_{comb} + Q_{rad} - Q_{conv} - Q_{evap} \quad (1)$$

Where equation (1) can be written in the following form;

$$dT/dt_{oil} = \frac{m_{gas}C_{pgas}(T_{in_{oil}} - T_{out_{oil}})}{V_{tank}\delta_{oil}C_{p_{oil}}} - \frac{m_{oil}C_{p_{oil}}(T_d - T_L)}{V_{tank}\delta_{oil}C_{p_{oil}}} \quad (2)$$

$$Q_{add} = 4.18 CV_{bio} m_{bio} \eta_{heater} \quad (3)$$

$$Q_{conv} = h_w A_{wall}(T_{gas} - T_{well}) \quad (4)$$

$$Q_{rad} = E_g A(T4_a - T4_{bed}) \quad (5)$$

$$Q_{evap} = \eta_{water} H_{evap} \quad (6)$$

$dT/dt_{oil}$: Represents the time-variation of the thermal oil temperature in the heat exchanger tank (see Figure.1).

The hot flue gas emitted from the incinerator combustion chamber is coupled with a thermal oil loop and Organic Rankine Cycle (ORC) to generate refrigerant superheated vapor at waste heat boiler as shown in Figure.1. Readers interested in further details on the Organic Rankine Cycle, (ORC), incinerators as well as their performances, thermodynamic and environmental properties of working fluids intended for ORC high temperature applications

ISSN: 2277-9655
Impact Factor: 4.116
CODEN: IJESS7

are advised to consult Sami [25,26]. In addition, other ORC applications have been comparatively assessed and presented in these references for use in low grade temperature waste heat Organic Rankine Cycle systems.

The following thermodynamic and energy conversion equations can be written to evaluate the performance of the ORC [25, 26, and 27];

$$W_{ORC} = m_{ref}(h_1 - h_2) \quad (7)$$

$$Q_{WHB} = m_{ref}(h_1 - h_4) \quad (8)$$

$$\eta_{ORC} = \frac{W_{ORC}}{Q_{WHB}} \quad (9)$$

Where; $W_{ORC}$, $Q_{WHB}$, $m_{ref}$, $\eta_{ORC}$, represent the work generated by the ORC vapor turbine, waste heat absorbed by the ORC at the waste heat boiler, mass flow rate of ORC refrigerant circulating in ORC and finally the conversion efficiency of ORC from waste heat to electrical energy, respectively.

Thermodynamic properties of enthalpies $h_1$, $h_2$, $h_3$ and $h_4$ at inlet, and outlet of vapor turbine, inlet and outlet waste heat boiler, respectively, outlined in equations (7) and (8) are calculated using REFPROP [25, 26].

**Solar Photovoltaic**

The solar photovoltaic panel is made of modules and each module is consisted of arrays and cells. The dynamic current output can be obtained as follows [13, 28];

$$I_p = I_L - I_o\left[\exp\left(\frac{q\,(V+I_p\,R_s)}{A\,k\,T_C}\right) - \left(\frac{(V+I_p\,R_s)}{R_{sh}}\right)\right] \quad (10)$$

And where,

$$Io = BT^3{}_C\left[\exp\left(-\frac{Ego}{K\,T_C}\right)\right] \quad (11)$$

$$I_L = P_1 G[1 - P_2(G - G_r) + P_3(T_C - T_r)] \quad (12)$$

It is worthwhile noting that the PV cell temperature $T_c$ is influenced by various factors such as solar radiation, ambient conditions, and wind speed. This parameter impacts the PV output current, and its time-variation and can be determined from the following [9, 13, and 23];

$$\left(m\,C_{p_{module}}\right)\frac{dT_C}{d_t} = Q_{in} - Q_{conv} - Q_{elect} \quad (13)$$

Where;

$$Q_{in} = \alpha_{abs} G S_p \quad (14)$$

$$Q_{conv} = S_p H(T_C - T_a) \quad (15)$$

$$Q_{elect} = \eta G S_C \quad (16)$$

$$H = 1.2475\,(\Delta T \cos\beta)^{\frac{1}{3}} + 2.685u \quad (17)$$

$$\eta = \eta_o[1 - \gamma(T_C - T_r)] \quad (18)$$

Where,

$Sp$, $G$, and $S_c$ are total surface area of the PV module, global solar radiation (w/m$^2$) and total surface area of cells in module, respectively.

**Battery charging and discharging Model:**

The battery stores excess power going through the load charge controller (CF Figure.1). The battery keeps voltage within the specified voltage and thus, protects over discharge rates, and prevent overload.

During the charging period, the voltage-current relationship can be described as follows [13, 24, and 29];

$$V = V_r + \frac{I\left(\frac{0.189}{(1.142-soc)+R_i}\right)}{AH} + (soc - 0.9)\ln\left(300\frac{I}{AH} + 1.0\right) \quad (19)$$

And;

$$V_r(V) = 2.094[1.0 - 0.001(T - 25°C)] \quad (20)$$

ISSN: 2277-9655
Impact Factor: 4.116
CODEN: IJESS7

However, during the discharging process and using equation (19), the current-voltage can be;

$$V = V_r + \frac{I}{AH}\left(\frac{0.189}{soc} + R_i\right) \quad (21)$$

And $R_i$ is given by;

$$R_i(\Omega) = 0.15[1.0 - 0.02(T - 25°C)] \quad (22)$$

Where,

$V_r(V)$ , I: the terminal voltage and current, respectively.

$R_i(\Omega)$ : Internal resistance of the cell and

$T$ is the ambient temperature.

$AH$: Ampere-hour rating of the battery during discharging process.

Finally, the power produced by the PV array can be calculated by the following equation,

$$P = V\, I_p \quad (23)$$

Where $I_p$ is given by equation (10).

**Charge Controller:**

Generally, the load charge controller power output is given by [13, 24, and 28];

$$P_{Cont-dc} = V_{bat}(I_{rect} + I_{PV} + I_{orc}) \quad (24)$$

Where; $V_{bat}$ is multiplication of the nominal voltage DC in the battery for any particular system and $I_{rect}, I_{PV}$ $and$ $I_{orc}$ represent the output current of the rectifier in DC and currents of PV and generator of the ORC vapor turbine.

**Inverter:**

The characteristics of the inverter are given by the ratio of the input power to the inverter $P_{inv-ip}$ and inverter output power$P_{inv-op}$. The inverter will incur conversion losses and to account for the inverter efficiency losses, $\eta_{inv}$ is used [13, 23, and 28];

$$P_{inv-ip}.\eta_{inv} = P_{inv-op} \quad (25)$$

The AC power of the inverter output P(t) is calculated using the inverter efficiency $\eta_{inv}$ , output voltage between phases, neutral $V_{fn}$, for single-phase current $I_o$ and $cos\varphi$ as follows;

$$P(t) = \sqrt{3}\,\eta_{inv} V_{fn} I_o\, cos\varphi \quad (26)$$

Finally, the hybrid system energy conversion efficiency for harnessing energy total P(t) from solar PV and Biomass/CHP-ORTC is given by;

$$\eta_{hybrid\ system} = \frac{P(t)}{Qin + Qadd} \quad (27)$$

Where; $Q_{in}$ and $Q_{add}$ are the solar irradiance and incinerator heat of combustion, respectively.

## NUMERICAL PROCEDURE

The energy conversion and heat transfer mechanisms taking place during various processes shown in the hybrid system as presented in Figure.1, are described by Equations (1) through (27). These equations have been solved as per the logical flow diagram presented in Figure. 2, where the input parameters of Biomass loading material, PV solar panel as well as the ORC thermodynamic characteristics and independent parameters are defined. Dependent parameters were calculated and integrated in the system of equations in finite-difference formulations. Iterations were performed until a solution is reached with acceptable iteration error. Then the solution of the systems of equations is competed and printed, program stopped.

ISSN: 2277-9655
Impact Factor: 4.116
CODEN: IJESS7

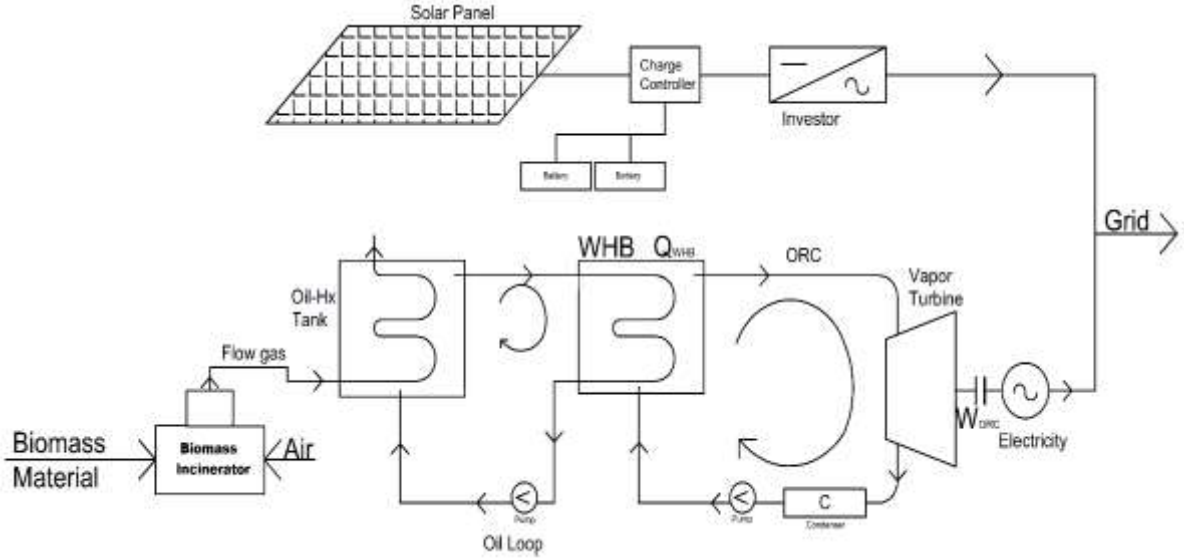


***Figure.1 Proposed hybrid system PV, Biomass and CHP***

The numerical procedure starts with using the solar radiation, biomass loading to calculate the mass flow rate of flue gas, thermal oil flow rate, and refrigerant flow rate circulating in various loops under specified conditions (C.F. Figures 1, 2). The thermodynamic and thermophysical properties of the flue gas, thermal oil, and refrigerant are determined based upon the initial conditions of the biomass incinerator loading, lower heating value, air flow rate, excess air ratio, and combustion products. This follows by using the finite-difference formulations to predict the time variation of PV cell temperature, oil tank temperature as well as other mass flow rates, hybrid system power outputs and individual efficiencies. Finally, the hybrid system efficiency is calculated at each input condition of the biomass incinerators and PV solar panels.

## RESULTS AND DISCUSSION

In order to solve the aforementioned conservation and conversion mass and energy balance equations (1) through (27) and taking into account that total power may not be simultaneous, and for validation purposes, this simulation model and the above mentioned equations were coded with finite-difference formulations. In addition, for the purpose of validation and tuning up the predicted output simulated results, the data was used to validate the simulation program under various conditions. In the following sections, we present analysis and discussions of the numerical results predicted as well as validations of the proposed simulation model.

Figures. 3 and 4 present a typical ambient temperature and solar isolation profiles at the site for various months of the year 2015 and 2016 at different hours of the day. It is quite apparent that the peak solar irradiation and maximum temperatures occur at midday; however, depending upon the daily solar radiation, the solar radiation may peak at different hours. It is worthwhile noting that the average monthly values of solar irradiation and ambient temperatures were used in the modeling and simulation of the Photovoltaic panels.

**Biomass Simulation:**

Equations (1) through (9) present the heat and mass heat balances at the combustion chamber where the solid waste is fed and process of combustion releases heat which is converted to the gas and ash through chemical reactions. Three loading of municipal solid waste (MSW) incinerators were considered for this study; 100, 150 and 200 t/d with lower heating values (LHV) of 1000, 1700 and 2300kcal/kg for the simulation. The low quality waste compositions for the simulation were 59% moisture, ash 8% and combustible 33% [15-18].The maximum excess air ratio was 1.76-2 for the waste of high quality (LHV=2300 kcal/kg) ) and the minimum excess air ratio was 1.05-1.26 for the waste of low quality (LHV=1000 kcal/kg). This is necessary to maintain the furnace temperature exit within the range of 850-950 °C to ensure complete combustion [15-18]. It is well known that increasing the excess air results in decreasing the combustion gas [16, 17], therefore, the minimum excess air ratio was selected at 1.05-1.26. Furthermore, it is also worthwhile mentioning that as reported by Yang et al. [17] carbon and hydrogen contents contribute to increase the heating value of waste material. In the municipal solid waste material selected the carbon and hydrogen contents were 14% and 2.24%, respectively.

ISSN: 2277-9655
Impact Factor: 4.116
CODEN: IJESS7

The predicted results of the biomass simulation at different conditions are presented in Figures 5 through 9. In particular, figures 5 and 6 depict the biomass output power at the ORC generator end and biomass energy conversion efficiency as function of the lower heating value (LHV) and flue gas flue rate for various waste loadings. It is quite evident from the data presented in these figures that waste material with higher LHV increases the output power and similarly higher flue gas flow rates increases the biomass output power. Similar behavior was observed at other waste material loadings. This has been observed by other studies in the literature [15-18].
In addition, the results displayed in Figures 5 and 6 show that the higher biomass loading and heat supplied the higher output power generated at the ORC. Since higher and lower temperatures conditions of the ORC's refrigerant at the waste heat boiler are controlled and remain unchanged, increasing the heat input and biomass loading at the incinerator increases the heat and temperature of the flue gases and consequently, the refrigerant mass flow rate produced (evaporated) at the waste heat boiler of the ORC and power output at the ORC (see Figure .1). Therefore, the higher biomass loading at the incinerator the higher the biomass output power and the biomass energy conversion efficiency. In addition, as previously discussed, higher the furnace gas exit temperature within 2250 F results in higher biomass efficiency; this is attributed to the complete combustion and the destruction of incomplete combustion products (ICP) and full burning. Furthermore, as pointed out the data also illustrates that the higher the biomass loading the higher the biomass efficiency.

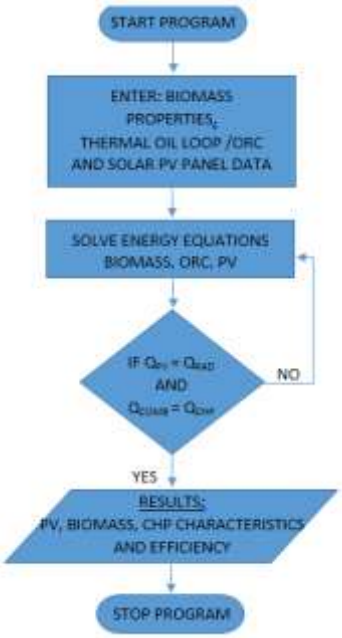


***Figure.2 Flow diagram of Hybrid system calculation***

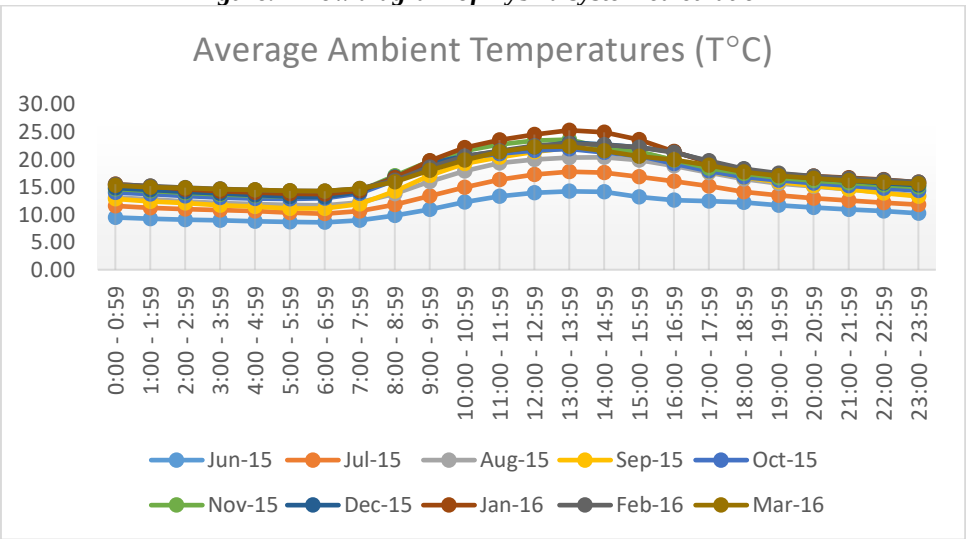


***Figure.3 Ambient temperatures (°C) profile 2015-2016***

ISSN: 2277-9655
Impact Factor: 4.116
CODEN: IJESS7

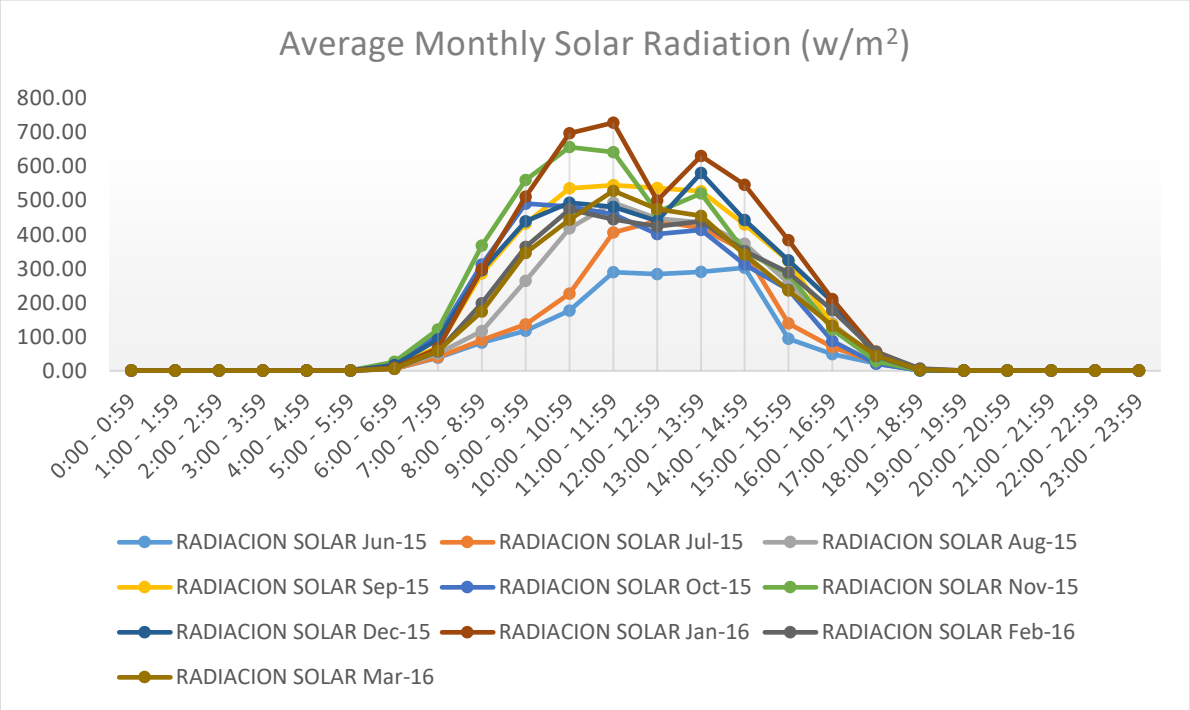


***Figure. 4 Solar irradiances (w/m$^2$) Profile 2015-2016***

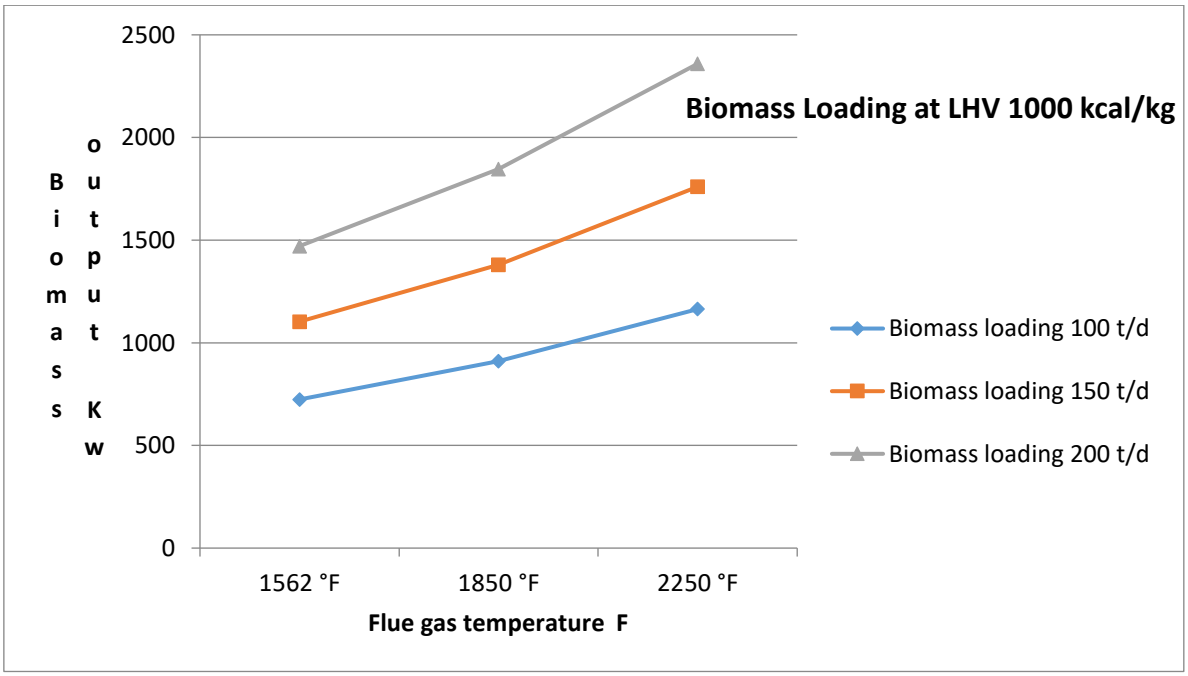


***Figure 5. Biomass output power at different biomass loading***

ISSN: 2277-9655
Impact Factor: 4.116
CODEN: IJESS7

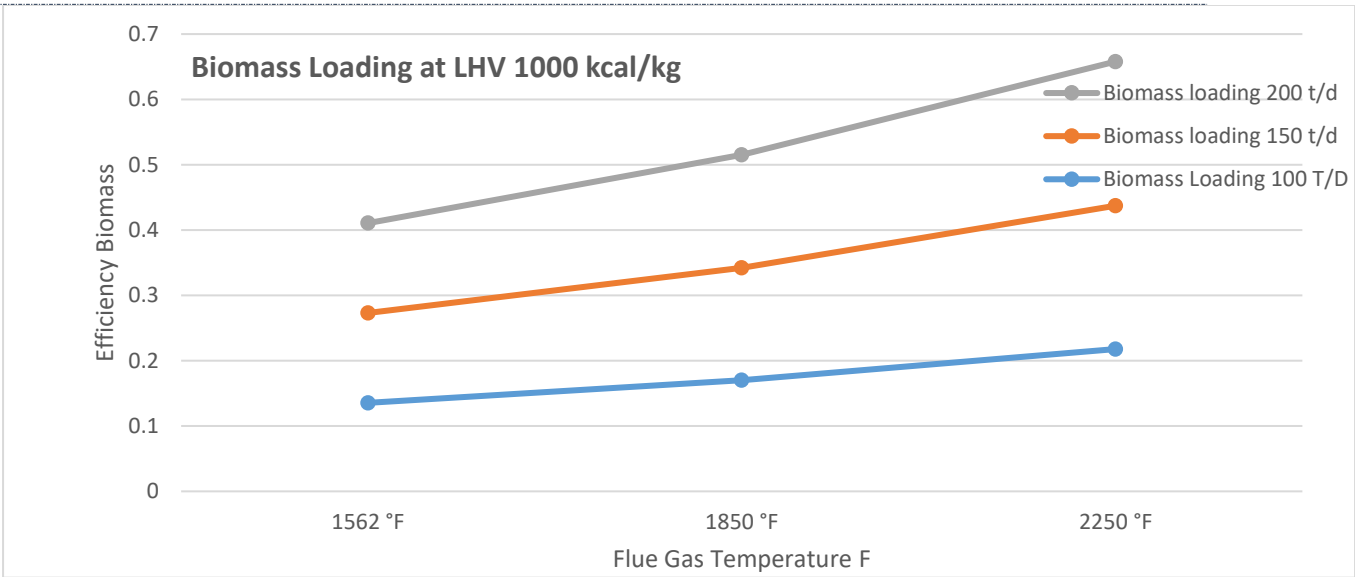


***Figure. 6 Biomass efficiency at different biomass loading***

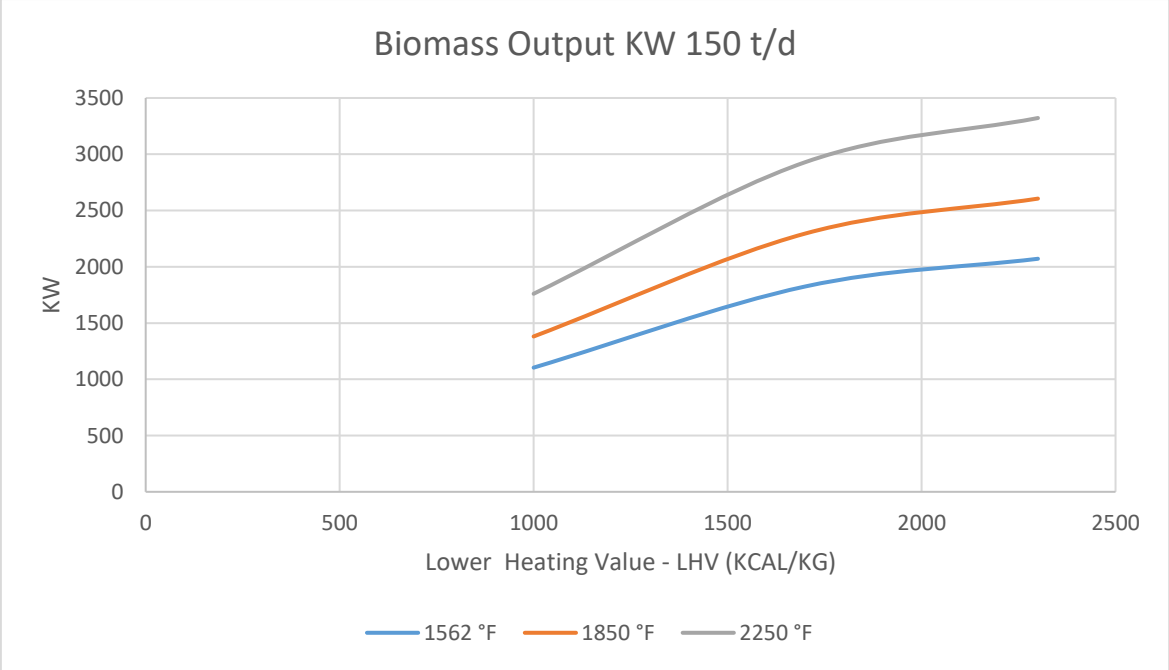


***Figure. 7 Biomass output power at different biomass loading***

ISSN: 2277-9655
Impact Factor: 4.116
CODEN: IJESS7

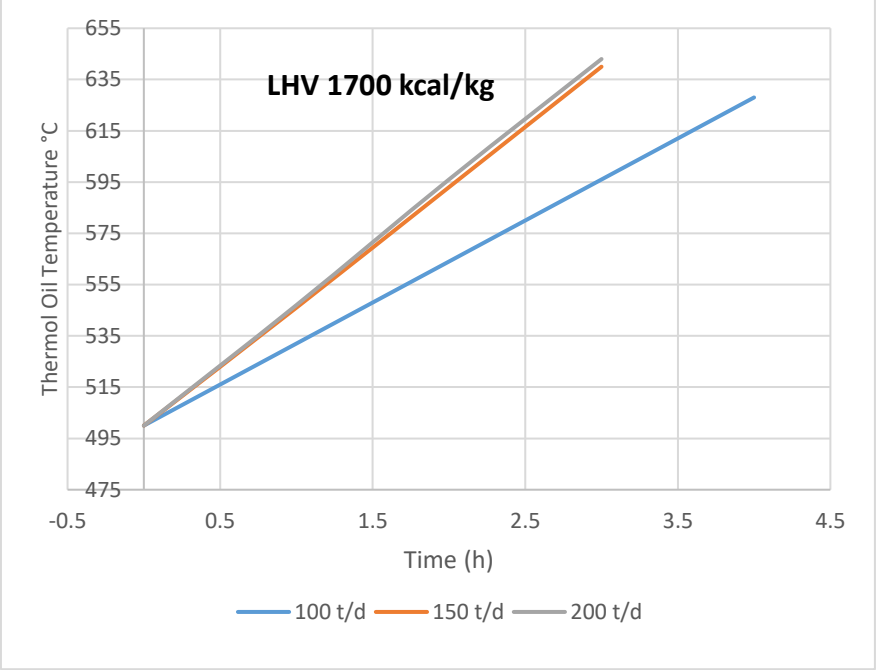


***Figure.8 Heat transfer fluid temperature at different biomass loadings***

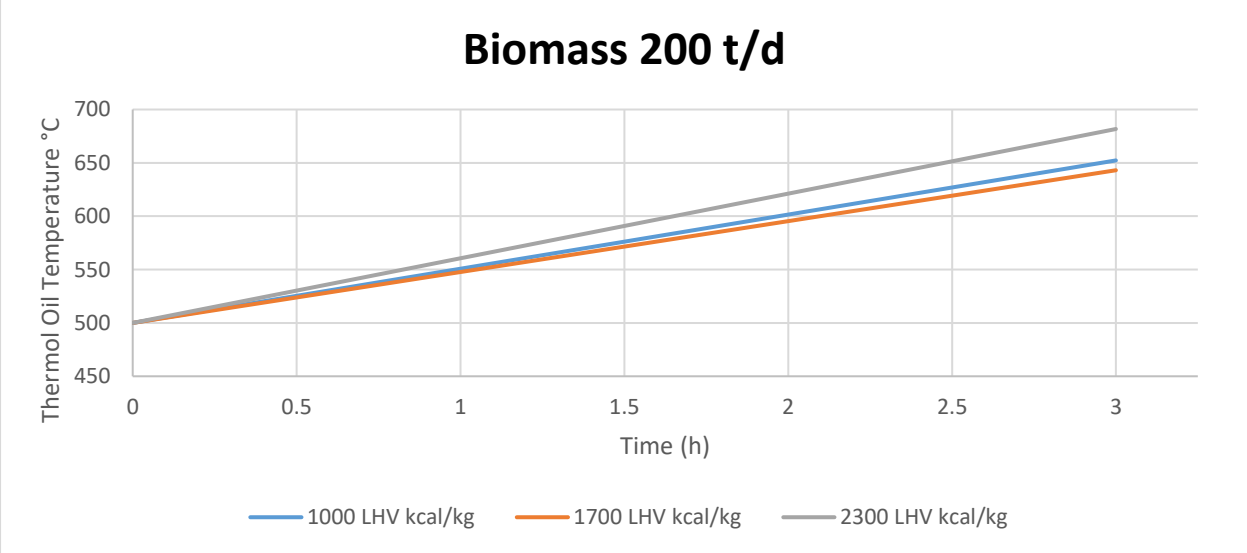


***Figure. 9 Heat transfer fluid temperature at different biomass fuel heating values***

The dynamic behavior of the heat transfer fluid; thermal oil medium to transfer the heat from the biomass flue gas to the ORC waste heat boiler can be predicted by equation (2) and results are shown in Figures 8 and 9 for various biomass loadings and heating values. It is quite clear from the data displayed in these figures that the maximum allowable temperature of the thermal oil was achieved on average after 3.5 hours. This is important since beyond this temperature the Dow thermal oil considered in this simulation could disintegrate and compromise the heat transfer process in the waste heat boiler and consequently negatively impacts the biomass power output at the ORC generator end as shown in Figure.1 and biomass system efficiency.

**PV Simulation:**

In the following sections, the basic concept and the characteristics of energy conversion process from the solar insolation into electrical energy, as shown in Figure.1, are presented and analyzed. This system is an integral part of the hybrid system under investigation. Figures 10 through 22 illustrate the characteristics of the process of the

ISSN: 2277-9655
Impact Factor: 4.116
CODEN: IJESS7

energy conversion from the solar radiation into electrical energy in terms of volts, amperes and power, solar irradiance and variation of PV cell temperatures as well as the efficiency of the Photovoltaic system.

It is worthwhile noting that the numerical simulation presented hereby was conducted under different conditions such as; PV cell temperatures from 10°C through 38°C, ambient temperatures from 10°C through 38°C and solar radiations from 400 to 1000 w/m$^2$ . Figures 10 and 11 present the energy conversion process characteristics as function of the solar radiation. It is also quite clear, in particular, from figures 10 and 11 that higher irradiance will result in higher energy conversion efficiency and higher output PV power. Therefore, it can be pointed out from these figures that the solar panels will be more efficient if operates at sites with higher solar irradiance. Similar conclusions have been reported in the literature [9, 13, and 24].

Furthermore, in order to study the impact of the initial PV cell temperature on the characteristics of the energy conversion process, Figures .12 through. 14 have been constructed. It is quite evident from Figure.12 that at a particular solar radiation, the higher the initial cell temperature the higher the PV power produced. This is significant since normally higher initial cell temperatures are associated with higher solar radiation as reported in the literature [9-14]. This particular characteristic can be easily demonstrated by equations (10) through (12). Furthermore, Figure. 13 presents the PV energy conversion efficiency for different initial cell temperatures and solar radiations. The data presented in this figure also illustrates that the higher the initial cell temperature, the higher the PV efficiency and consequently higher PV power. This again provide strong evidence that the solar panels will be more efficient if operate at sites with higher solar irradiance

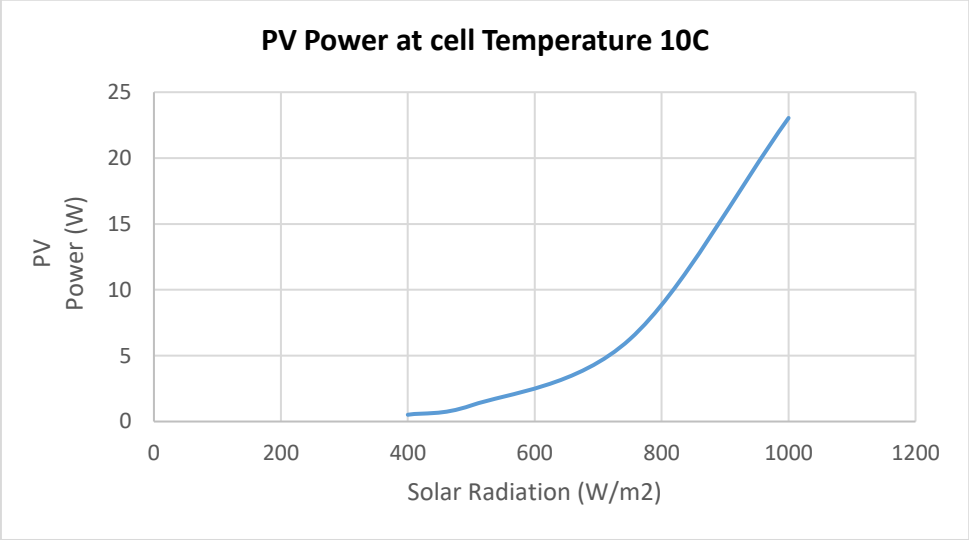


***Figure. 10 PV Power for different values of irradiance- W/m2***

ISSN: 2277-9655
Impact Factor: 4.116
CODEN: IJESS7

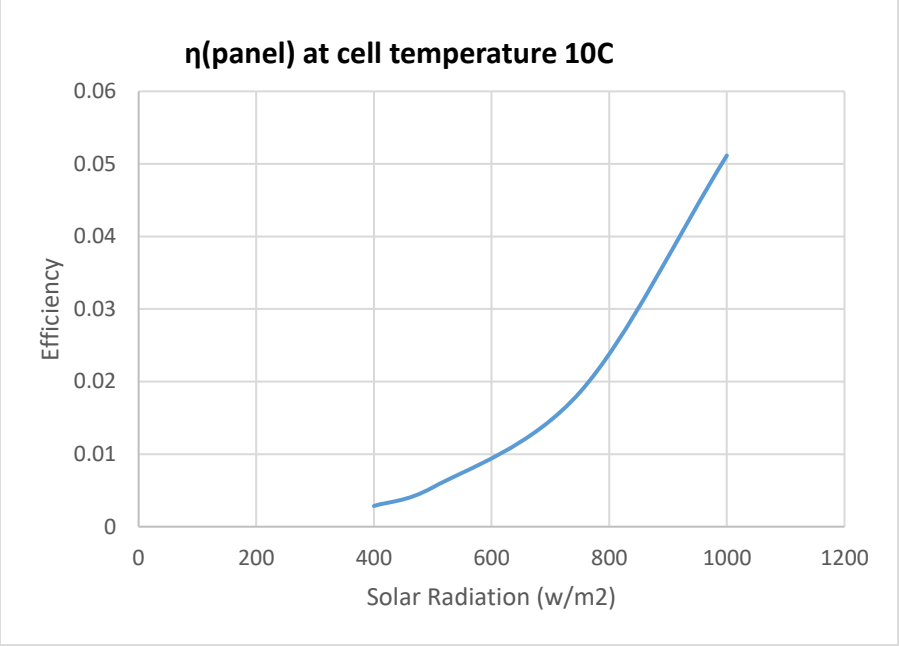


***Figure. 11 PV efficiency for different values of irradiance- W/m²***

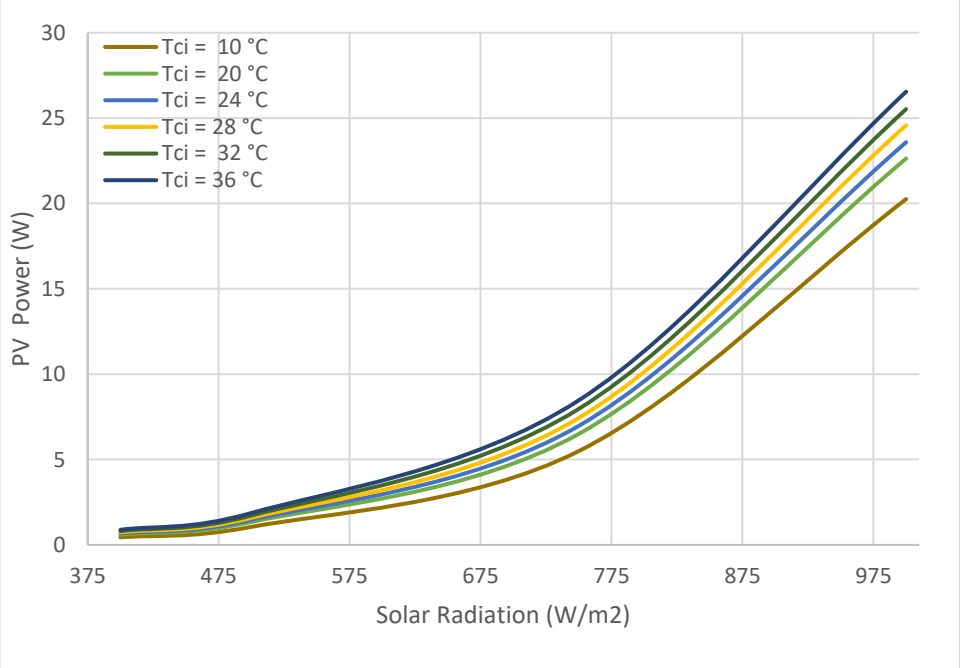


***Figure. 12 PV Power for different values of irradiance- W/m²***

ISSN: 2277-9655
Impact Factor: 4.116
CODEN: IJESS7

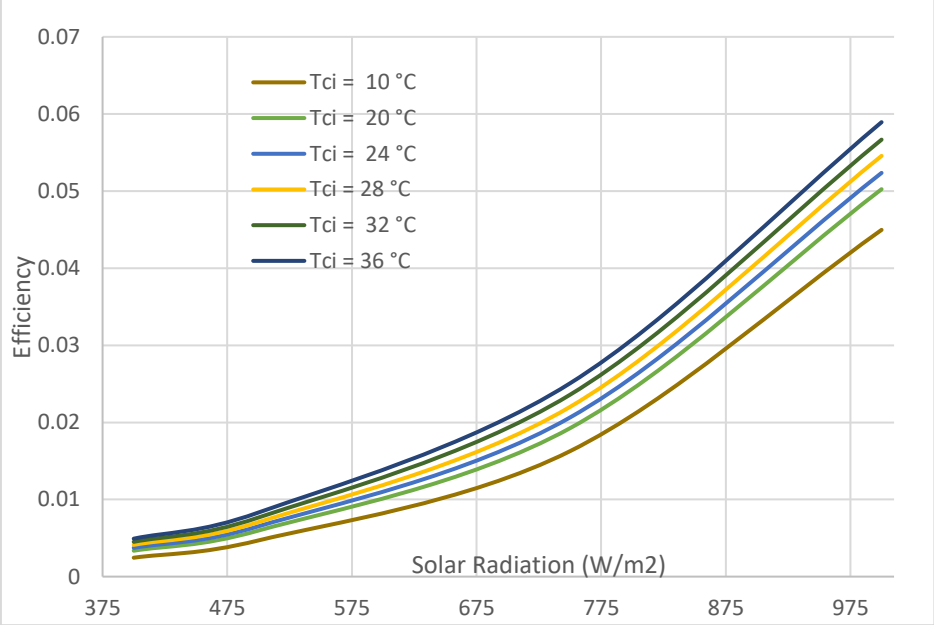


***Figure. 13 PV efficiency for different values of irradiance- W/m2***

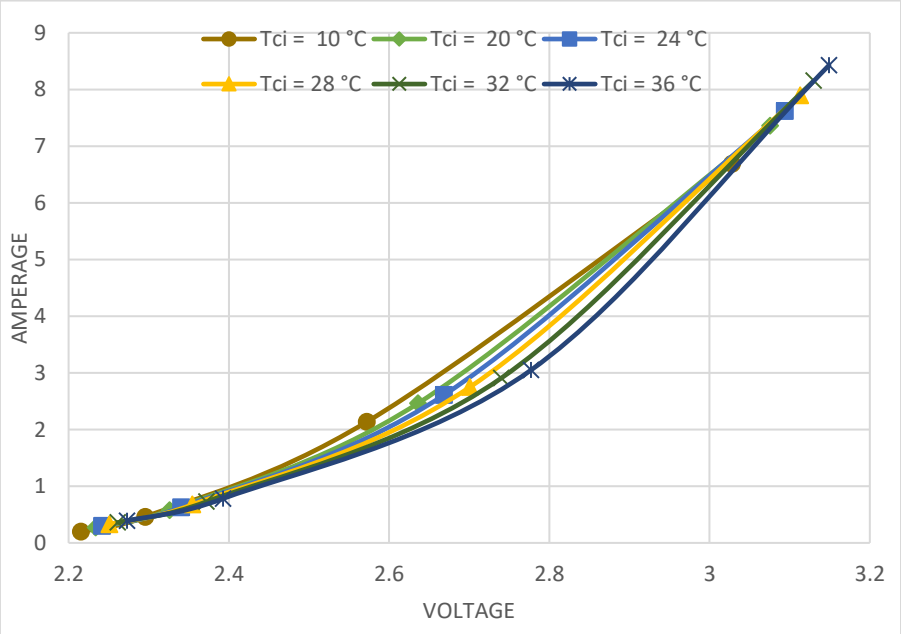


***Figure. 14 PV Amperage for different PV cell initial temperature***

ISSN: 2277-9655
Impact Factor: 4.116
CODEN: IJESS7

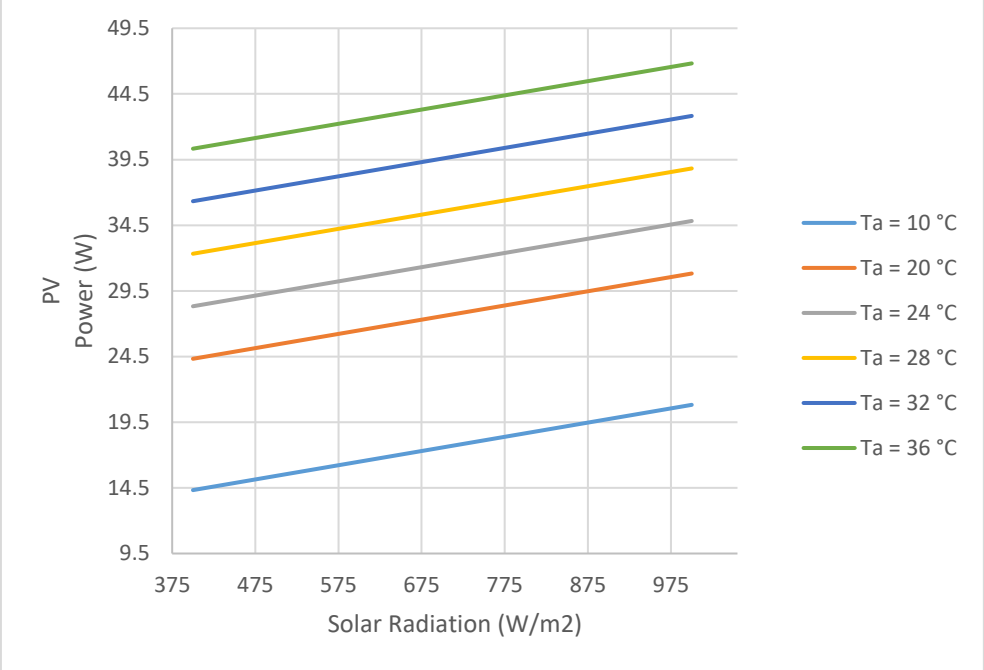


***Figure. 15 PV Power for different values of irradiance- W/m2***

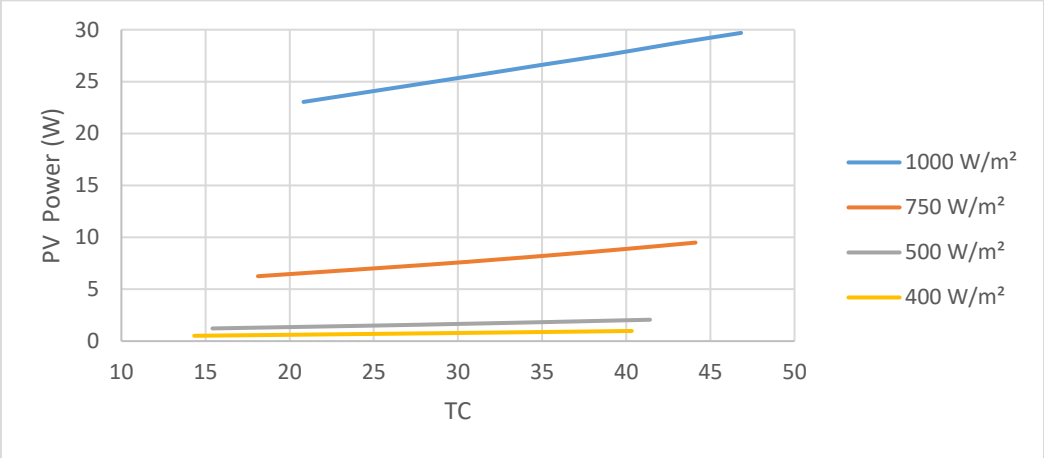


***Figure. 16 PV Power for different PV cell temperature***

Further, one of the most important characteristics of the solar PV is the ampere- voltage profile. Therefore, Figure. 14 has been constructed and presented to illustrate the impact of initial cell temperature on the PV panel amperage where the data show that the higher the initial cell temperature the higher the output PV amperage at rated voltage. However, the results displayed in this figure showed for the type of PV under investigation [13] that at voltage higher than 3 volt, the PV output capacity is insignificantly influenced by the initial cell temperature.

Furthermore, we have learned from the literature [9-14] that it is important not only the PV cell temperature is impacted by solar radiation but also by the ambient temperature, therefore, Figures 15 and 16 have been presented to illustrate the effect of the ambient temperature on the PV output power at various solar radiation and cell temperatures. It has been previously shown by equations (10) through (12) that the PV output power is influenced by the cell temperature, ambient temperature as well as the solar radiation. The results presented in Figures. 15 and 16 clearly showed that at a particular solar radiation, the higher the ambient temperature the higher the PV power produced. In addition, Figure.16 showed and confirmed that the higher the PV cell temperature and the radiation the higher the solar PV power produced.

ISSN: 2277-9655
Impact Factor: 4.116
CODEN: IJESS7

In addition, the results of the solution of equations (13) through (15) together with the other equations of the PV simulation model are presented in Figure.17 for the time-variation of the PV cell temperature, under various solar radiations. It is apparent from the results displayed in this figure that at a particular time, the higher the solar radiation the accelerated increase in the PV cell temperature. The maximum temperature is achieved at higher solar radiation of 1000 w/m$^2$ within 1400 seconds. As pointed out earliest and illustrated in equation (13), the dynamic behavior of the PV cell temperature depends mainly upon the PV material and solar radiation.

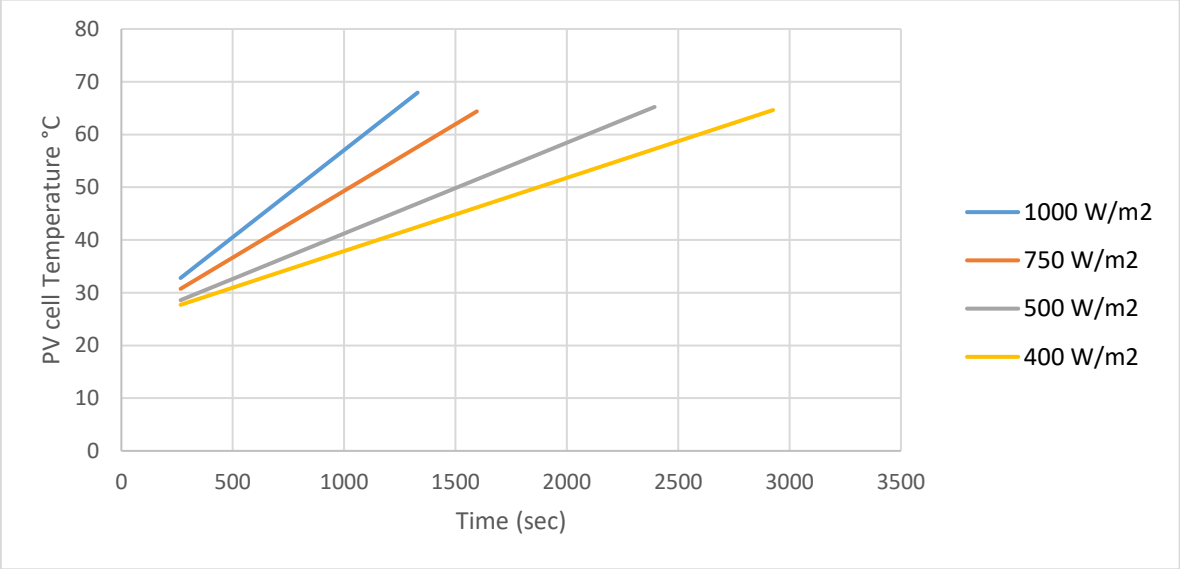


***Figure. 17 Time variation of PV cell temperature at different solar radiations***

As mentioned, since the PV solar panel dynamic behavior depends upon solar radiation and ambient conditions, it is important in the selection and design of PV solar panel to know the daily hourly variation of the ambient conditions; solar radiation and ambient temperature (C.F Figures 3 and 4). Therefore, the hourly daily variation of the solar radiation, PV power, efficiency as well as the PV amperage are presented in Figures 18 through 21 for June 2015, January 2016 and February 2016 for comparison purposes. The data presented in these figures were the averages values of each parameter during each month at specific daily hour as shown in the figures. It is quite evident from these figures that the PV power, efficiency and amperages have the same trend as the hourly variation of the solar radiation. This trend is expected since the PV power, amperage and PV solar conversion efficiency are fully impacted and dependent upon the solar radiation hourly profile. This has been reported in the literature [9, 13, and 24].

As also the data displayed in these figures point out that, in general, the peak of the PV power and amperage occurs at the peak of the solar radiation around the mid-day, however, as per Figure 4, depending on daily solar radiation, the peak may be at different hours. Consequently, the higher the solar radiation the higher the PV power, PV amperage and PV efficiency.

Therefore, it is imperative that the designer of the PV panel takes into consideration the daily variation of the PV cell temperature, and solar radiation as well as the ambient temperatures and the fact that solar panels will be more efficient when operated at sites with higher solar irradiance.

ISSN: 2277-9655
Impact Factor: 4.116
CODEN: IJESS7

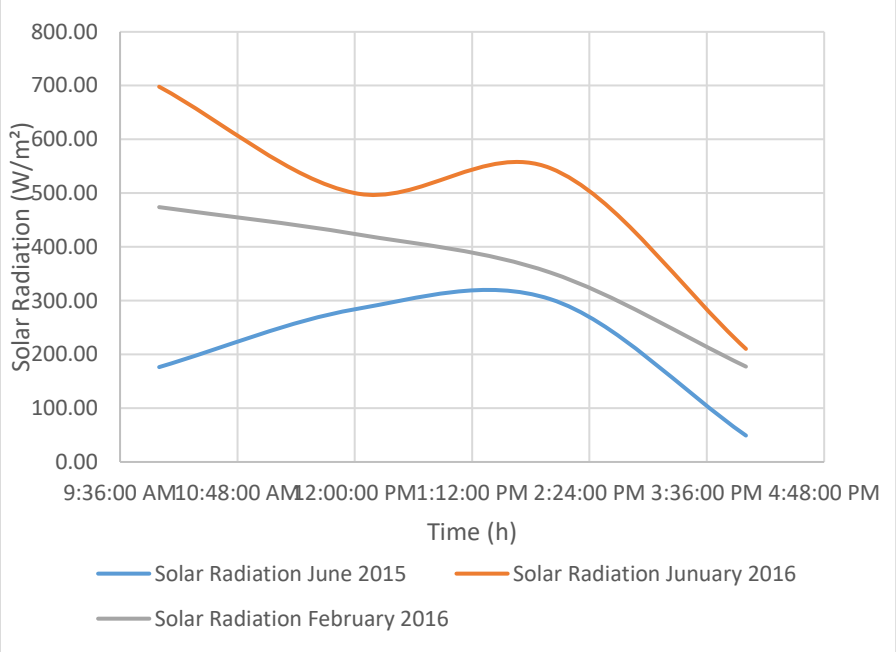


***Figure. 18 Hourly solar radiation for 2015 and 2016.***

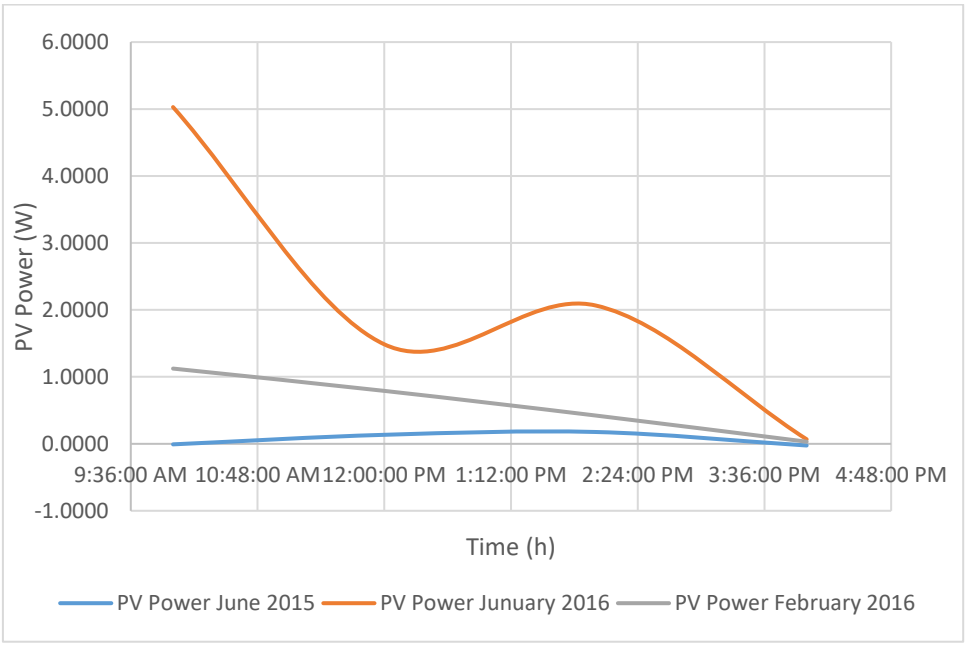


***Figure. 19 Variation of PV power hourly***

ISSN: 2277-9655
Impact Factor: 4.116
CODEN: IJESS7

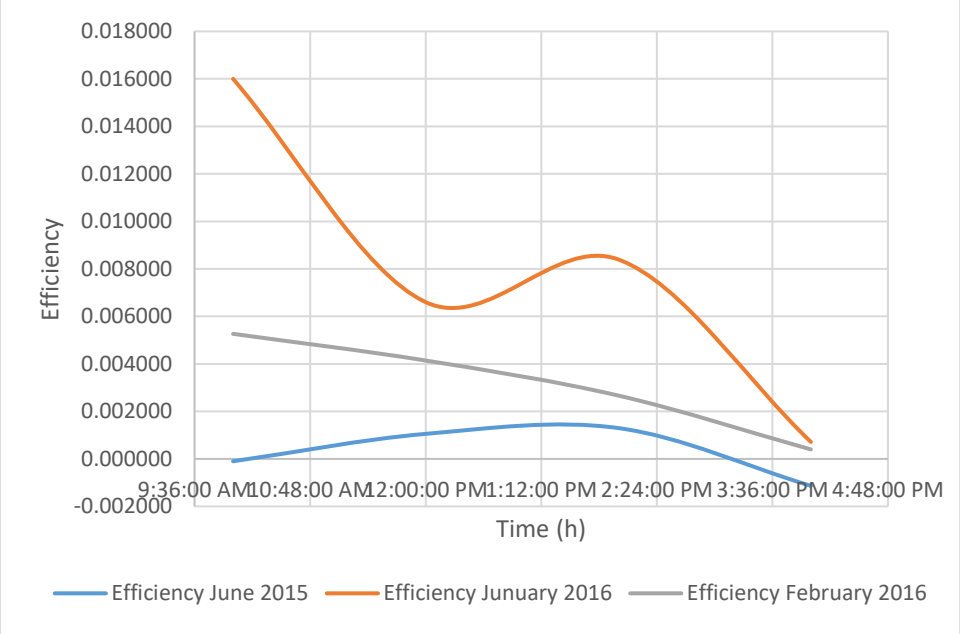


***Figure. 20 Variation of PV solar panel efficiency***

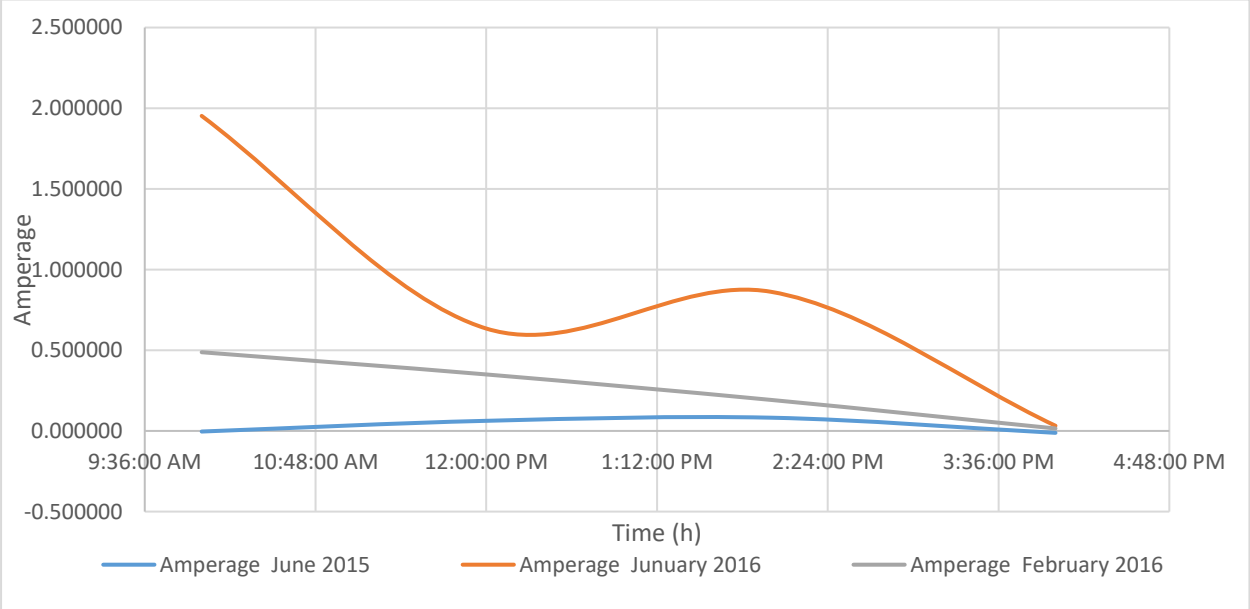


***Figure. 21 Variation of PV Amperage hourly***

ISSN: 2277-9655
Impact Factor: 4.116
CODEN: IJESS7

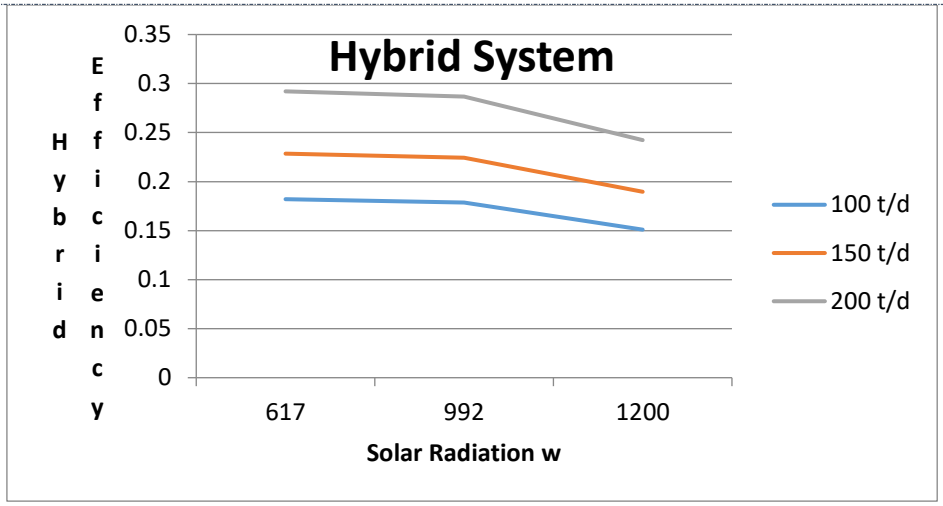


*Figure 22 Variation of hybrid system efficiency at different solar radiation*

**Simulation of Hybrid System:**

Finally, Figure 22 has been constructed to illustrate the impact of the energy input sources on the hybrid under investigation composed of solar PV and biomass/CHP subsystems such as the solar radiation and the municipal waste loadings on the output power and consequently the efficiency of the hybrid system. It was assumed in this particular simulation that the total electrical load delivered by the hybrid system is shared between the biomass and solar PV by 60% and 40%, respectively. The results displayed in this figure clearly show that at a particular solar radiation, higher biomass loading (t/d) results in higher hybrid system efficiency. Furthermore, the results also illustrate that higher solar radiation increases power delivered by the hybrid system, however, reduces the hybrid system efficiency due to the increase of the input energy. In our opinion, this is attributed to the fact that the higher and lower temperatures conditions of the ORC's refrigerant at the waste heat boiler are controlled and remain unchanged, and the energy conversion efficiency of the PV solar panels is lower than that of the Biomass /ORC CHP efficiency.

**Validation of Simulation Model:**

In order to validate our numerical model prediction described in equations (1 through 27), we have constructed Figures 23 and 25 to compare the predicted results with data presented in the literature for biomass and solar PV. It is quite apparent from Figure 23 that the model prediction fairly compares with the data of Yang et al. [16 and 17] at various biomass loadings. However, analyzing Figure 23 points out that our model predicted very well the biomass data up to loading of 150t/d and beyond that point there were some discrepancies between the model prediction and the data. We believe these discrepancies are due to the fact that data on high biomass loading was not fully disclosed and discussed in references [16 and 17] and our model could not take into account the heat transfer losses at higher biomass loadings.

Another attempt to validate our model's prediction where, predicted PV solar characteristics; power and amperage [23] were compared with data presented by reference [30] and presented in Figure.24. Comparison between the experimental Data [30] and the mathematical model prediction at 750W/$m^2$ has demonstrated that the model fairly predicted the data of Ramon et al. [30].

ISSN: 2277-9655
Impact Factor: 4.116
CODEN: IJESS7

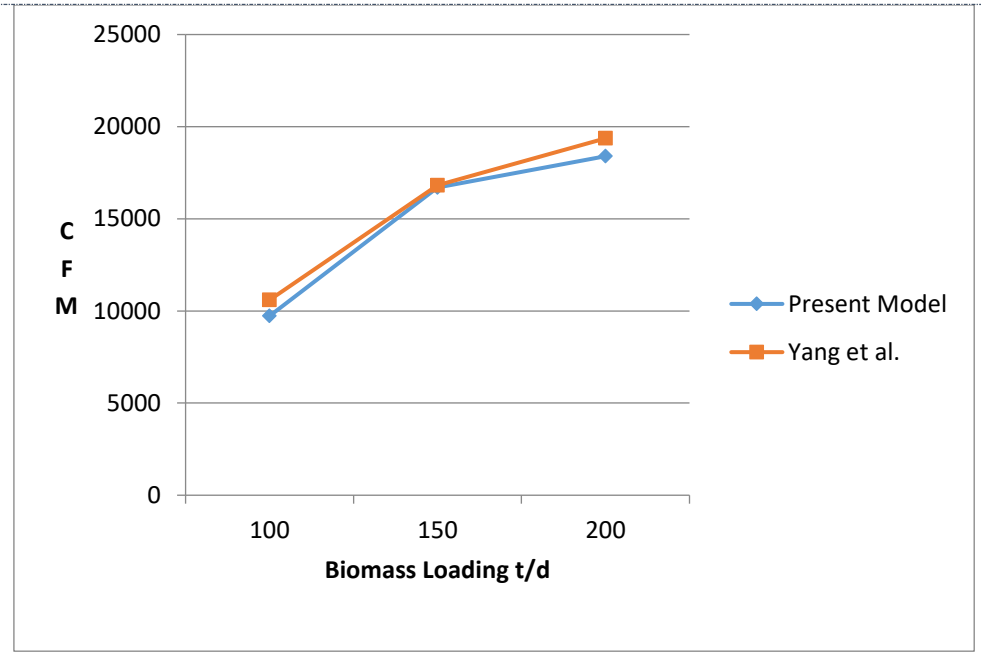


***Figure. 23 Comparison with Data Yang et al. [16, 17] at different biomass loadings (t/d)***

On the other hand, the prediction of dynamic cell temperature profile by the formulation presented in the PV simulation model was compared to the data presented by Fagali et al. data [13] in Figure. 25. The comparison presented in this figure showed that the model and data have the same trend, however, some discrepancies exist. It is believed that the discrepancies are due to the fact that Fagali et al. [13] did not provide full disclosure of the various parameters used in equations (10) and (11) and Reference Rajapakse, A et al. [29] had to be consulted on the various missing parameters in Fagali et al. [13]. However, taking into account the complexity of the PV cell temperature phenomena and its thermal behavior, we feel that our model fairly predicted the PV cell dynamic profile.

## CONCLUSIONS

The energy conservation and conversion equations describing the total power generated by a hybrid system of solar photovoltaic, biomass integrated ORC-combined heat and power cycle have been developed, coded, analyzed, solved and presented. The biomass data illustrates that the higher the biomass loading, the higher the power and efficiency. Furthermore, the PV study results showed that the higher the solar radiation, the accelerated increase in the PV cell temperature and consequently, the higher the solar radiation the higher the PV power and PV amperage. It is imperative that designers of the PV panel and its cell temperature take into consideration the solar radiation as well as the ambient temperatures. Finally, the model prediction compared fairly with the biomass and PV data at different conditions.

ISSN: 2277-9655
Impact Factor: 4.116
CODEN: IJESS7

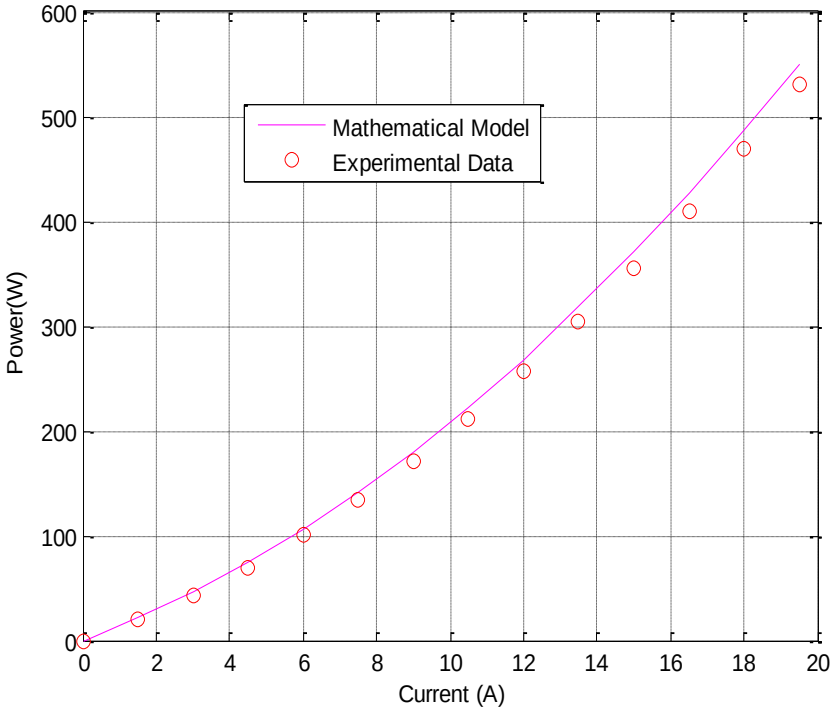


*Figure. 24 Comparison of Current model [23] and Experimental Data [30] at 750W/m².*

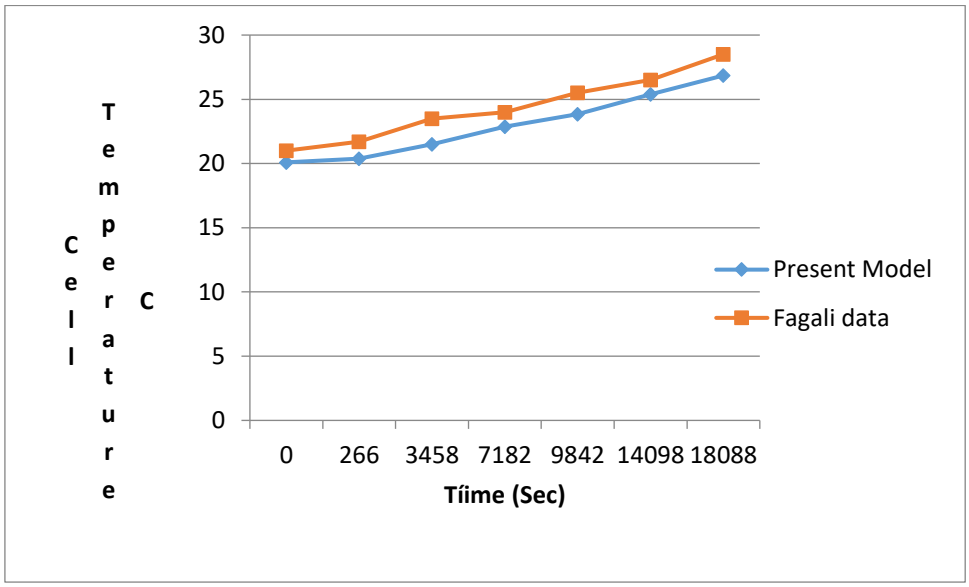


*Figure 25.- Comparison of Current model and Experimental Data [13].*

**Nomenclature:**

$A_{pvg}$ = PV solar collector area ($m^2$)

A: Radiation surface area.
$B$: Device and material constant
$C_{p_{oil}}$: Specific heat of thermal oil
$C_p$: Specific heat of Flue gas
$CV_{bio}$: Calorific heat value of bio-gas

ISSN: 2277-9655
Impact Factor: 4.116
CODEN: IJESS7

$E_g$: Stefan Boltzmann Coefficient
$E_{go}$: Band gap Energy at 0 K
$G$: Solar radiation (w/m$_2$)
$G_r$: Reference radiation (w/m$^2$)
$h_w$: Convection heat transfer coefficient
$h_1$: Enthalpy of refrigerant at vapor turbine entrance
$h_2$: Enthalpy at exit of vapor turbine
$h_4$: Enthalpy at inlet of waste heat boiler
$H$: Convective heat transfer coefficient
$I_p$: Output current of PV panel.
$I_o$: Reverse saturation current and is a function of the cell temperature as per equation (11).
$I_L$: Load current
$m\ C_{p_{module}}$: Effective thermal capacity of the PV module
$P_1$, $P_2$, $P_3$ are constants
$Q_{in}$: Solar energy absorbed by the module
$Q_{conv}$: Energy loss due to convection
$Q_{elect}$: Electric power produced
$Q_{comb}$: Combustion heat added
$Q_{rad}$: Radiative heat
$Q_{conv}$: Convective heat
$Q_{evap}$: Evaporative heat
$Sp$: Total surface area of PV module
$T_C$: The cell temperature (K)
$T_r$: Reference temperature (K)
$\Delta T$: Temperature difference ($T_c$-$T_a$)
$(T_C - T_r)$: Difference between reference temperature (298 K) and cell temperature.
$u$: Wind speed
V: The output voltage of the PV array and approximately equal to the battery voltage.
$V_{tank}$: Volume of tank heater
$m_{gas}$: Mass flow rate of flue gas
$m_{bio}$: Biomass waste mass material
$m_{ref}$: Mass flow rate ORC cycle refrigerant
$W_{ORC}$: Work generated at ORC vapor turbine generator
$Q_{WHB}$: Heat transferred from thermal oil to refrigerant at the waste boiler heat exchanger
T: is the temperature thermal oil in heat exchanger tank

**Greek alphabet**
$\alpha_{abs}$ : Overall absorption coefficient
$\beta$: Tilt angle
$\rho_{air}$= Air density.

$\eta_o$: Module efficiency at reference temperature (298 K)
$\eta_{inv}$= Inverter efficiency

$\eta_{ORC}$: ORC thermal efficiency
$\eta_{bio}$: Biomass furnace efficiency
$\gamma$: Coefficient for photovoltaic conversion efficiency

**Subscripts:**

$bat -$ Battery
$inv - ip$ - Inverter input
$inv - op$ - Inverter output
p – Power
PV – Photo Voltaic

$total$ – Total
$3f$ – Three phase AC

## ACKNOWLEDGEMENT

The research work presented in this paper was made possible through the support of the Catholic University of Cuenca.

## REFERENCES

1. Peterseim JH, White S, Tadros A, Hellwig U." Concentrating solar power hybrid plants -Enabling cost effective synergies. Renew Energy; vol. 67:pp178 –85, 2014.
2. Zhang HL, Baeyens J, Degreve J, Caceres G. "Concentrated solar power plants: review and design methodology". Renew Sustain Energy Review, vol.22, 201.
3. Peterseim. J. H, Hellwig. U, Tadros. A, White. "Hybridisation optimization of concentrating solar thermal and biomass power generation facilities", Science direct Solar Energy vol. 99, pp. 203– 214, 2014.
4. Srinivas. T, Reddy.B.V, "Hybrid solar -biomass power plant without energy storage", Reference: CSITE22, Appeared in: Case Studies in Thermal Engineering, 23 January 2014.
5. Iftekhar,H., C.M. Duffy, A. and Norton, B. , "A Comparative Technological Review of Hybrid CSP-Biomass CHP Systems in Europe", International Conference on Sustainable Energy & Environmental Protection, Paisley, UK, 11-14 August, 2015
6. Department of Energy, "Potential Benefits of Distributed Generation and Rate Related Issues that may Impede their Expansion, A Study Pursuant to Section 1817 of the Energy Policy Act of 2005" 2007.
7. Binayak, B., Shiva, R. P., Kyung-Tae L., Sung-Hoon A., "Mathematical Modeling of Hybrid Renewable Energy System: A Review on Small Hydro-Solar-Wind Power Generation", International Journal of Precision engineering and Manufacturing-green Technology, Vol. 1, No 2, pp. 157-173, 2014.
8. Sirasani, K., Kamdi, S.Y.,"Solar Hydro Hybrid Energy System Simulation" International Journal of Soft Computing and Engineering (IJSCE), Volume-2, Issue-6, pp. 500-503, January 2013.
9. Mustafa E., "Sizing and Simulation of PV-Wind Hybrid Power System", International Journal of Photoenergy, Volume 2013, ID 217526, pp.1-10, 2013.
10. Akikur, R.K., Saidur, R., Ping, H., Ullah, K.R., "Comparative Study of Stand-Alone and Hybrid Solar Energy Systems Suitable for Off-Grid Rural electrification: A review", Renewable and Sustainable Energy Reviews, Vol. 27, 738-752, 2013.
11. Bhandari, B. "Design and Evaluation of tri-hybrid Renewable System (THRES)," Ph. D. Thesis, Department of Mechanical & Aerospace Engineering, Seoul National University, 2014.
12. Saha, N.C., Acharjee, S., Mollah, M.A.S., Rahman, K.T., and Rafi, F. H. M.," Modeling and Performance Analysis of a Hybrid Power System", Proc. of International Conference on Informatics Electronics & Vision (ICIEV), pp. 1-5, 2013.
13. Fargali, H., M., Fahmy, F.H. and Hassan, M.A., "A Simulation Model for Predicting the Performance of PV/Wind- Powered Geothermal Space Heating System in Egypt", The Online Journal on Electronics and Electrical Engineering (OJEEE), Vol.2, No.4, 2008.
14. Mahalakshmi, M., and Latha, S. "Modeling, Simulation and Sizing of Photovoltaic/Wind /Fuel Cell Hybrid Generator System", International Journal of Engineering Science and Technology, Vol 4, No 5, 2012.
15. Choi, S., Lee, J.S., Kim, S.K. and Shin, D.H., "Comparative Evaluation of Municipal Solid Waste Incinerators Design by Flow Simulation", Combustion & Flame, Vol 106, 241-251, 1996.
16. Yang, W, Shin, D., and Choi, S." A Process Simulation Model for a 2 ton/hr Incinerator (A Combined Bed Combustion and Furnace Heat Transfer Model), International Journal of Energy Research, Vol.22, Issue 11, 943-951, 1998.
17. Yang, W., Nam, Hyung-sik and Choi, S., "Improvement of Operating Conditions in Waste Incinerators using Engineering Tools", Waste Management, Vol 27,604-613, 2007
18. Gan, S., Goh, Y.R., Calkson, P.J., Parracho, A., Nasserzadeh, V. and Swithenbank, J. ," Formation and Elimination of Polychlorinated Dibenzo-p-Dioxins and Polycholrinated Debenzofurans from Municipal Solid Waste Incinerators", Combustion Science and Technology Vol.175, 103-124. 2013.
19. Deissler, G "Diffusion approximation for thermal radiation in gases with jump boundary conditions" ASME Journal of Heat Transfer, Vol 86, 240-246, 1964.
20. Bekele, G and Tadesse, G., " Feasibility Study of Small Hydro/Pv/Wind Hybrid System for off- Grid Rural Electrification in Ethiopia", Applied Energy, Vol 97, pp.5-15, 2012.

ISSN: 2277-9655
Impact Factor: 4.116
CODEN: IJESS7

21. Fadaeenejed, M, Radzi, M. A., AbKadir, M.Z. and Hizam, H.," Assessment of Hybrid Renewable Power Sources for Rural Electrification in Malaysia", Renewable and Sustainable Energy Reviews, Vol. 30, pp. 299- 305, 2013.
22. Saha, N.C., Acharjee, S., Mollah, M.A.S., Rahman, K.T., and Rafi, F. H. M.," Modeling and Performance Analysis of a Hybrid Power System", Proc. of International Conference on Informatics Electronics & Vision (ICIEV), pp. 1-5, 2013.
23. Dewangan, A.K., "Modeling and Simulation of Photovoltaic Full Cell Hybrid System", International Journal of Engineering Research and Technology, Vol 3, Issue 2, 2014.
24. Sami, S. and Icaza, D. "Modeling, Simulation of Hybrid Solar Photovoltaic, Wind turbine and Hydraulic Power System", IJEST, International Journal of Engineering Science and Technology, Volume 7, Issue 9, September 30, 2015.
25. Sami, S., "Behaviour of ORC low Temperature Power Generation with Different Refrigerants" International Ambient Energy Journal, Volume 32, No.1, 2011
26. Sami, S.M., "ORC for low Temperature Power Generation with low GWP Refrigerants" International Ambient Energy Journal, iFirst, 1-7, 2012
27. **Sami, S., and Marin, E. "A Numerical Model for Predicting Dynamic Performance of Biomass-Integrated Organic Rankine Cycle, ORC, System for Electricity Generation", AJEE, American Journal of Energy Engineering, Volume 4, No 3, p 26-33, 2016.**
28. Howell, J.R., Bannerot, R.B., Viet, G.C."Solar-Thermal Energy Systems: Analysis and Design, Modeling of photovoltaic module and experimental determination of serial resistance" McGraw-Hill, Inc., New York, 1982
29. Rajapakse, A, Chungpaibulpantana, S., "Dynamic simulation of a photovoltaic refrigeration system". RERIC, Vol. 16 (3), 67-101, 1994.
30. Murugan, N, Umamaheswari, M., Vimal, SI, and Sivashanmugam,P. " Experimental Investigation on Power Output in Aged Wind Turbines", Advances in Mechanical Engineering, Volume 2012, Article ID 380986, 7 pages, July 2015.
31. Ramon, A, Lopez, A, Maritz, A and Angarita, G, " Parametros comparatives de celulas fotoelectricas para generaciob de energia: implementacion de banco de pruebas usando DSP comparative parameters of solar cells for power generation: test stand implementation using DSP". Ingeniería Energética Vol. XXXV, 3/2014 p. 193- 201, Septiembre/Diciembre ISSN 1815 – 5901, 2014